STIC-ILL

RL 261. A1 C15

From: Portner, Ginny
Sent: Thursday, September 14, 2000 12:55 PM
T : STIC-ILL
Subject: edb

10269

A pilot pharmacokinetic and immunoscintigraphic study with the technetium-99m-labeled monoclonal antibody BC-1 directed against oncofetal fibronectin in patients with brain tumors.
Mariani G; Lasku A; Pau A; Villa G; Motta C; Calcagno G; Taddei GZ; Castellani P; Syrigos K; Dorcaratto A; Epenetos AA; Zardi L; Viale GA
Nuclear Medicine Service, DIMI, University of Genoa, Italy.
Cancer (UNITED STATES) Dec 15 1997, 80 (12 Suppl) p2484-9, ISSN 0008-543X Journal Code: CLZ
Languages: ENGLISH
Document type: JOURNAL ARTICLE

Ginny Portner
Art Unit 1645
CM1-7e13
(703) 308-7543

BEST AVAILABLE IMAGES

Defective images within this document are accurate representation of The original documents submitted by the applicant.

Defects in the images may include (but are not limited to):

- BLACK BORDERS
- TEXT CUT OFF AT TOP, BOTTOM OR SIDES
- FADED TEXT
- ILLEGIBLE TEXT
- SKEWED/SLANTED IMAGES
- COLORED PHOTOS
- BLACK OR VERY BLACK AND WHITE DARK PHOTOS
- GRAY SCALE DOCUMENTS

IMAGES ARE BEST AVAILABLE COPY.

As rescanning documents *will not* correct images, please do not report the images to the Image Problem Mailbox.

Sixth Conference on Radioimmunodetection and Radioimmunotherapy of Cancer

Supplement to Cancer

A Pilot Pharmacokinetic and Immunoscintigraphic Study with the Technetium-99m–Labeled Monoclonal Antibody BC-1 Directed against Oncofetal Fibronectin in Patients with Brain Tumors

Giuliano Mariani, M.D.[1]
Arben Lasku, M.D.[1]
Antonio Pau, M.D.[2]
Giuseppe Villa, M.D.[1]
Cinzia Motta, M.D.[1]
Giuseppina Calcagno, M.D.[1]
Gioconda Z. Taddei, M.D.[1]
Patrizia Castellani, Ph.D.[3]
Kostas Syrigos, M.D.[4]
Alessandra Dorcaratto, Ph.D.[2]
Agamennon A. Epenetos, Ph.D.[4]
Luciano Zardi, Ph.D.[3]
Giuseppe A. Viale, M.D.[2]

[1] Nuclear Medicine Service, DIMI, University of Genoa, Genoa, Italy.

[2] Institute of Neurosurgery, University of Genoa, Genoa, Italy.

[3] Laboratory of Cell Biology, Istituto Nazionale per la Ricerca sul Cancro (IST), Genoa, Italy.

[4] Hammersmith Hospital, London, United Kingdom.

BACKGROUND. Preliminary experiments in an animal model have shown the favorable tumor targeting potential in vivo of radiolabeled BC-1, an immunoglobulin (Ig)G_1 monoclonal antibody (MoAb) that recognizes the human fibronectin isoform (B^+) containing the ED-B oncofetal domain. This antigen has extremely restricted distribution in normal adult tissues. Instead, it is highly expressed in fetal and tumor tissues, especially in high grade astrocytomas and malignant gliomas of the brain, in which the process of neoangiogenesis linked to tumor growth is particularly important.

METHODS. This study was carried out with five patients who had malignant brain tumors (four gliomas and one malignant angioblastic meningioma). The BC-1 MoAb was labeled with technetium-99m (^{99m}Tc) by MDP transchelation. Planar and single photon emission computed tomography (SPECT) imaging was acquired at 4–6 and 20 hours after intravenous injection of about 450 MBq/0.2 mg ^{99m}Tc-BC-1 and was compared with the nonspecific indicator of blood-brain barrier disruption, ^{99m}Tc–diethylenetriamine pentaacetic acid (DTPA). Plasma pharmacokinetic analysis was based on serial blood sampling. All patients underwent potentially curative surgery at the end of the study.

RESULTS. The plasma clearance curves were biexponential, with average $T_{1/2}$ values of 2–4 hours and 28–33 hours, respectively. ^{99m}Tc-BC-1 showed very low nonspecific uptake in the bone marrow, liver, and spleen. Planar and SPECT imaging with ^{99m}Tc-BC-1 visualized brain tumors in all patients, with a pattern of intratumor distribution that specifically identified areas of peripheral tumor growth more accurately than the nonspecific indicator, ^{99m}Tc-DTPA. Tumor uptake of ^{99m}Tc-BC-1 was correlated with the expression of the specific oncofetal fibronectin, as shown by immunohistochemistry on surgical samples.

CONCLUSIONS. These results indicate the diagnostic potential of MoAb ^{99m}Tc-BC-1 for immunoscintigraphy in cancer patients, at least when neoangiogenesis induced by cancer is particularly important. *Cancer* **1997;80:2484–9.**

KEYWORDS: immunoscintigraphy, oncofetal fibronectin, monoclonal antibody, brain tumors, radiopharmacokinetics.

Presented in part at the 43rd Annual Meeting of the Society of Nuclear Medicine, Denver, Colorado, June 3–5, 1996; the European Nuclear Medicine Congress, Copenhagen, Denmark, September 14–18, 1996; and the Sixth Conference on Radioimmunodetection and Radioimmunotherapy of Cancer, Princeton, New Jersey, October 10–12, 1996.

Supported in part by grants from the Associazione Italiana per la Ricerca sul Cancro (AIRC), Milan, Italy, and the National Research Council of Italy (CNR), Rome, Italy (Progetto Finalizzato: Applicazioni Cliniche della Ricerca Oncologica).

Dr. Lasku is the recipient of a fellowship from the International Atomic Energy Agency (IAEA), Vienna, Austria. Dr. Lasku's current address is: Nuclear Medicine Center, University Hospital Center, Tirana, Albania.

Address for reprints: Giuliano Mariani, M.D., Nuclear Medicine Service, DIMI, University of Genoa, Viale Benedetto XV, n. 6, I-16132 Genoa, Italy.

Received August 12, 1997; accepted September 5, 1997.

Preliminary experiments in nude mice bearing human tumor implants have shown the favorable tumor targeting potential of the monoclonal antibody (MoAb) BC-1, a murine immunoglobulin (Ig) of the IgG_1 subclass.[1] This MoAb recognizes the (B^+)-fibronectin isoform containing the ED-B oncofetal domain, a sequence originated by alternative splicing.[2-9]

Fibronectins, the members of a family of adhesive glycoproteins with high molecular mass that are present in the extracellular matrix and in body fluids,[10] are involved in a number of biologic events, including wound healing and oncogenic transformation.[11] To a certain degree, fibronectin polymorphism is due to alternative splicing patterns in three regions (IIICS, ED-A, and ED-B) of the single primary transcript, and is also due to post-translational modifications. The altered splicing pattern of fibronectin-pre-mRNA occurring in transformed cells and in malignancies leads to increased expression of fibronectin isoforms containing the IIICS, ED-A, and ED-B sequences.[3,4,6,12-15]

The (B^+)-fibronectin specifically recognized by MoAb BC-1 has extremely restricted distribution in normal adult tissues (except in regenerating endometrium). Instead, it is highly expressed in fetal and tumor tissues; it can therefore be identified as a novel "oncofetal" antigen in addition to being a marker of angiogenesis.[8,9,14]

The aim of this study was to explore the tumor targeting potential of radiolabeled MoAb BC-1 in cancer patients based on prior results obtained with the iodine-125-labeled BC-1 in the animal model of human tumor implants,[1] which indicated that high expression of oncofetal fibronectin during neoangiogenesis induced by cancer provides the biologic basis for specific accumulation of radioactivity in the tumor mass. For this purpose, the pharmacokinetic and scintigraphic imaging parameters of technetium-99m (^{99m}Tc)-labeled MoAb BC-1 were evaluated in patients with malignant brain tumors, a condition in which the process of neoangiogenesis linked to tumor growth is particularly important.[8,9]

MATERIALS AND METHODS

Patients

Five patients with malignant brain tumors were studied (3 women and 2 men; age range, 32-58 years). Four of the patients had brain gliomas and one had an angioblastic meningioma. All patients gave informed consent to the investigation, and all underwent surgery (with curative intent) at the end of the pharmacokinetic and immunoscintigraphic study. Resected tumor specimens were processed for immunohistochemistry with MoAb BC-1, to evaluate in the individual patients the pattern of oncofetal fibronectin expression as related to neoangiogenesis induced by tumor growth.

Radiopharmaceuticals

Purified MoAb BC-1 was kindly supplied by Antisoma, Ltd. (London, United Kingdom) as a sterile, pyrogen free solution of reduced antibody (0.5 mg in 0.5 mL) and was kept frozen at −20 °C until use. ^{99m}Tc-labeling was performed by a two-step MDP transchelation procedure, as follows: 1) a 35 μL aliquot from an Amerscan® MDP vial (Amersham International plc, Amersham, United Kingdom), reconstituted with 2 mL of 0.9% saline, was added to a thawed antibody vial and mixed gently; 2) freshly eluted ^{99m}Tc (925-1110 MBq, or 25-30 mCi) was then added, mixed, and incubated for 5-10 minutes at room temperature. The radiolabeling antibody mixture was then subjected to size-exclusion gel chromatography through Sephadex G-25 M (prepacked PD-10 columns supplied by Pharmacia Biotech AB, Uppsala, Sweden), which invariably showed a single radioactivity peak eluted in the protein elution zone. After further sterilization through a 0.22 μm Millipore filter, the final dose injected into patients was about 450 MBq/0.2 mg (or 12 mCi/0.2 mg) of ^{99m}Tc-BC-1. Prior experiments performed with ^{99m}Tc-BC-1 and ^{125}I-BC-1 employing enzyme-linked immunosorbent assay (ELISA) and radioimmunoassay (RIA) on solid-phase antigen had shown similar immunoreactivity for both radiolabels, whereas concomitant ELISA tests similarly performed on solid-phase antigen had demonstrated that the two radiolabeled antibodies had immunoreactivity equivalent to that shown by the cold, unlabeled MoAb BC-1.

Protocol of the Study

^{99m}Tc-BC-1 was injected intravenously (i.v.) as a single bolus, and heparinized venous blood samples were taken at frequent intervals until 48 hours after tracer injection, for pharmacokinetic analysis of the plasma clearance curves.

Planar and single photon emission computed tomography (SPECT) imaging of the head was acquired at 4-6 hours, whereas planar imaging only was acquired 20 hours after i.v. injection of ^{99m}Tc-BC-1. A gamma camera with a large field of view equipped with a general-purpose, parallel-hole collimator was employed, utilizing a 20% window centered on the 140 kiloelectron volt gamma emission peak of ^{99m}Tc. Reconstruction of SPECT images (60 steps over 360° in a 64 × 64 matrix, 30 seconds per step) was performed utilizing standard algorithms for attenuation correction and back-projection filtering. Whole body scintigraphic acquisitions were also routinely recorded at 6 and 24 hours after injection of ^{99m}Tc-BC-1. Two days before starting the ^{99m}Tc-BC-1 imaging and pharmacokinetic protocol, both planar and SPECT images of the head were acquired about 1 hour after the i.v. injection of ^{99m}Tc-diethylenetriamine pentaacetic acid (DTPA),

which was considered a nonspecific indicator of blood-brain barrier disruption.

Immunohistochemical Procedures

For immunohistochemical studies, 5 μm thick cryostat sections obtained from the tumors immediately after surgical resection were air-dried and fixed in cold acetone for 10 minutes. Immunostaining was performed with a streptavidin-biotin alkaline phosphatase complex staining kit (Bio-Spa Division, Milan, Italy) and naphtol-AS-MX-phosphate and Fast-Red TR (Sigma, St. Louis, MO) to visualize binding sites.

The reaction sequence consisted of the application of the primary MoAb (BC-1) and incubation with biotinylated goat-antimouse IgG and then with avidin-biotinylated peroxidase complex. The red reaction product was obtained by the use of a mixture of 2 mg naphtol AS-MX phosphate (Sigma) dissolved in 200 μL of n,n-dimethylformamide (Sigma) and diluted in 9.8 mL of 0.1M Tris-HCl buffer (pH 8.2) and 1mM levamisole (Sigma). Immediately before use, 10 mg of Fast-Red TR salt (Sigma) was added. Gill's hematoxylin was used as a counterstain, followed by mounting in glycergel (Dako, Carpenteria, CA).

A modified immunohistochemistry procedure was also applied, in that the reaction sequence was started with incubation with the biotinylated goat-antimouse IgG, without prior incubation with the antioncofetal fibronectin MoAb BC-1. This assessed the capability of the immunohistochemical system of detecting deposition of the radiolabeled MoAb in the tumor upon its administration in vivo.

RESULTS

Pharmacokinetic Evaluation

The decay-corrected plasma clearance curves of ^{99m}Tc-BC-1 were biexponential, with average biologic $T_{1/2}$ values of 2–4 hours for the early, fast component and 28–33 hours for the terminal, slow component (Fig. 1, top panel). The fraction of total activity represented by the back-extrapolated slow component was equal to 51.8 ± 8.4%. The plasma disappearance curves observed in the individual patients showed very consistent homogeneous patterns of clearance in three patients, whereas two patients exhibited somewhat different pharmacokinetic behavior. In particular, a slower clearance was observed in Patient AD01, simply due to partial extravasation of the injected radiopharmaceutical (as clearly shown by persistent radioactivity accumulation detected on the whole body scans at the antecubital injection site). In contrast, Patient MC04 exhibited a frankly faster plasma clearance curve than all the other patients studied. In this case, whole body scans exhibited a pattern of distribution in the skeletal structures (not shown), suggesting that

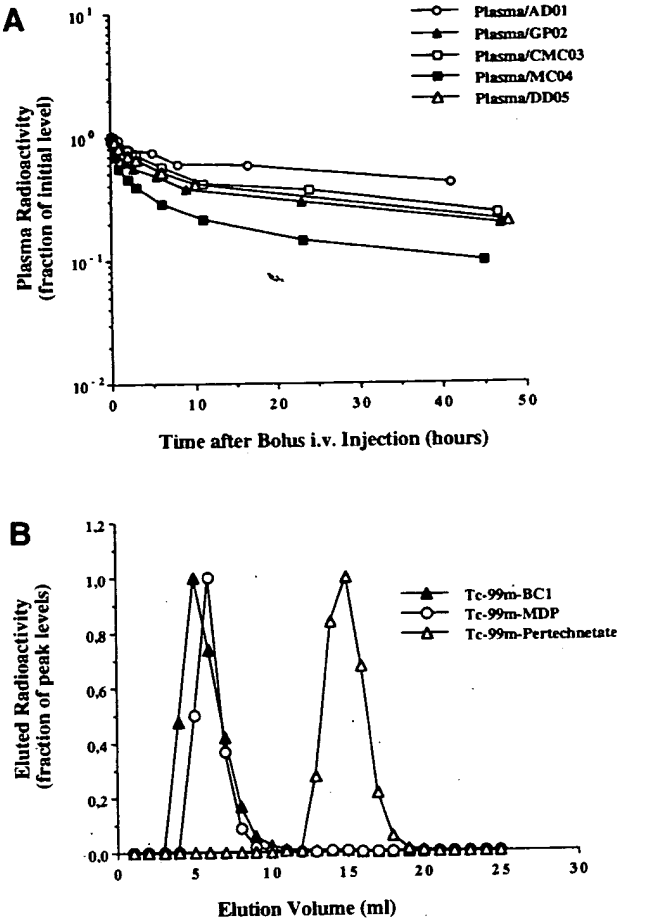

FIGURE 1. (A) Semilogarithmic plots of the plasma radioactivity disappearance curves observed in the five patients included in the ^{99m}Tc-BC-1 study are shown. The slower rate of disappearance observed in Patient AD01 was due to partial extravasation of the tracer at the injection site. The faster clearance rate observed in Patient MC04 was associated with a whole body scintigraphic pattern that suggested the presence of a fraction of ^{99m}Tc-MDP in the injected dose. (B) Radioactivity elution profiles obtained after gel chromatography through Sephadex G-25 M columns (PD-10) of aliquots containing ^{99m}Tc-BC-1, ^{99m}Tc-MDP, and ^{99m}Tc-pertechnetate, respectively, are shown. Because of incomplete MDP transchelation, chromatography was not capable of separating the radiolabeled antibody from the bone-seeking agent that could have been present in the labeling mixture.

this particular radiopharmaceutical preparation was characterized by incomplete MDP transchelation during the radiolabeling reaction. In fact, subsequent experiments showed that, although Sephadex G-25 M chromatography was clearly capable of purifying the ^{99m}Tc-labeled antibody from unreacted free ^{99m}Tc-pertechnetate, it could not purify ^{99m}Tc-BC-1 from any ^{99m}Tc-MDP that could have been produced during the labeling reaction (Fig. 1, bottom panel). On the other hand, Sephadex chromatography rules out the presence of radiolabeled particulate micelles in the injectate as a possible cause of radioactivity accumula-

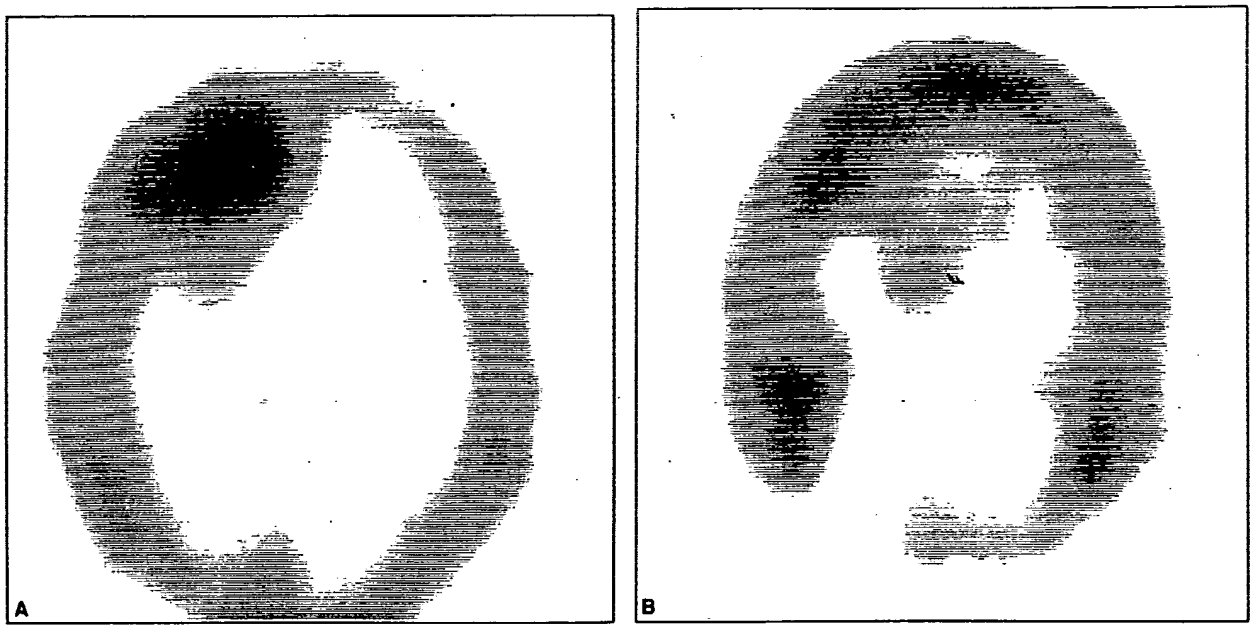

FIGURE 2. Patient MC04, who presented with bulky glioma of the right frontal lobe, is represented. (A) A transaxial single photon emission computed tomography (SPECT) section obtained after injection of the nonspecific indicator of blood-brain barrier disruption, ^{99m}Tc-diethylenetriamine pentaacetic acid, shows a very homogeneous pattern of distribution throughout the entire tumor. (B) A transaxial SPECT section obtained after injection of ^{99m}Tc-BC-1 is shown. The pattern of radiolabeled monoclonal antibody uptake outlines the peripheral rim of tumor growth, also extending to areas not yet involved by disruption of the blood-brain barrier.

tion in the bone marrow upon i.v. administration, which would produce in vivo scintigraphic imaging similar to that obtained with a bone-seeking agent, such as ^{99m}Tc-MDP.

Whole body scintigraphic imaging indicated very low nonspecific radioactivity uptake in the bone marrow, liver, and spleen at 6 and 24 hours after injection of ^{99m}Tc-BC-1 (not shown).

Scintigraphic Imaging

Planar and SPECT imaging with ^{99m}Tc-BC-1 made brain tumors clearly visible in all patients, showing a pattern of intratumor distribution that specifically identified areas of peripheral tumor growth more accurately than the nonspecific indicator of blood-brain barrier disruption, ^{99m}Tc-DTPA. This different pattern of intratumor radioactivity distribution (better identified by SPECT imaging) was obvious both in the patients with brain gliomas (Fig. 2) and in the single patient with a malignant angioblastic meningioma, in whom, as expected, radioactivity uptake was particularly intense for both radiopharmaceuticals.

In particular, scintigraphic observations made in the patient with angioblastic meningioma showed that the different patterns of radioactivity distribution could be attributed to specific binding of ^{99m}Tc-BC-1 rather than simply to poorer diffusion in the tumor mass of this macromolecule versus ^{99m}Tc-DTPA. In fact, although SPECT imaging with ^{99m}Tc-DTPA showed a clear delineation of the area of blood-brain barrier disruption induced by the tumor, imaging with ^{99m}Tc-BC-1 showed a halo of radioactivity uptake extending beyond the area of blood-brain barrier disruption indicated by ^{99m}Tc-DTPA, and this radioactivity uptake could have been linked to neoangiogenesis induced at the growing peripheral rim of the tumor (Fig. 3).

Immunohistochemical Analysis

Immunohistochemistry of the resected tumor specimens with MoAb BC-1 appeared to correlate tumor uptake of ^{99m}Tc-BC-1 directly with the degree of expression of the specific oncofetal fibronectin in different areas of the tumors (Fig. 4). On the other hand, the modified immunohistochemical procedure based on incubation of the tumor sections with the goat-antimouse IgG only failed to show in vivo deposition of detectable amounts of MoAb BC-1 after injection of the radiolabeled tracer (not shown).

DISCUSSION

The results of this study suggest that the radiolabeled MoAb BC-1 has potential as an in vivo tumor targeting agent in the treatment of cancer patients, at least when their conditions are strongly characterized by neoangiogenesis that is induced by tumor growth and also permits it. It should also be noted that the human tumor models

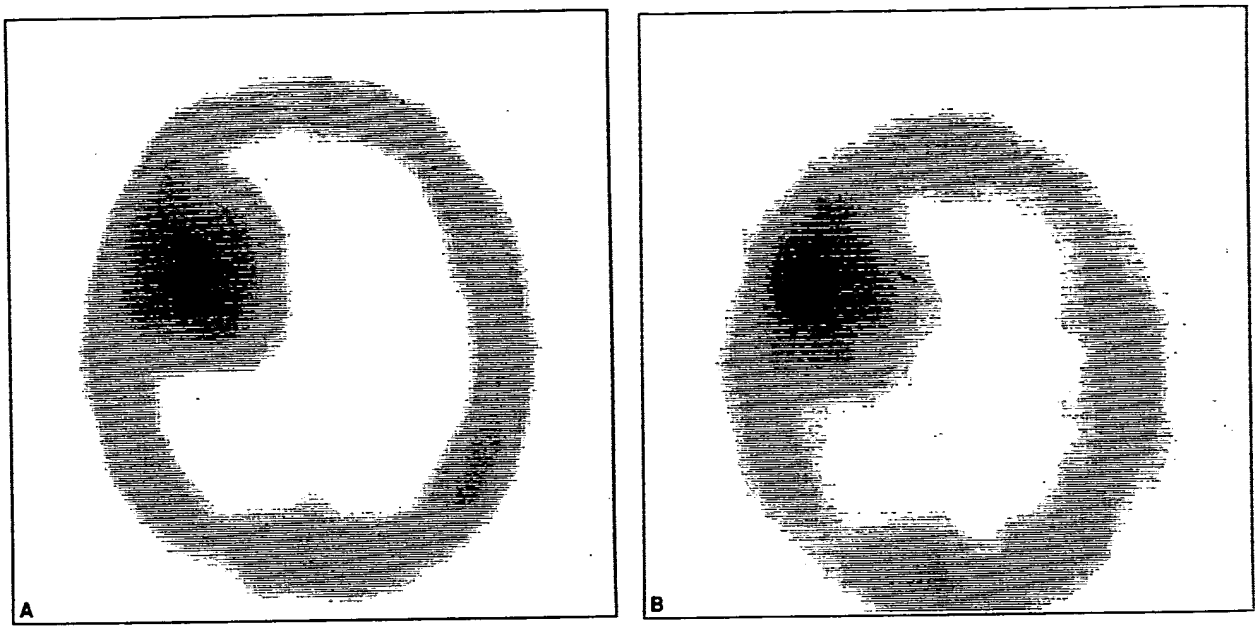

FIGURE 3. Patient GP02, who presented with bulky angioblastic meningioma of the right frontoparietal region, is represented. (A) A transaxial single photon emission computed tomography (SPECT) section obtained after injection of the nonspecific indicator of blood-brain barrier disruption, ^{99m}Tc-DTPA, shows intense uptake and a uniform pattern of distribution throughout the entire tumor. (B) A transaxial SPECT section obtained after injection of ^{99m}Tc-BC-1 is shown. Compared with the nonspecific indicator of blood-brain barrier disruption, ^{99m}Tc-DTPA, the scan obtained with ^{99m}Tc-BC-1 delineates more accurately the inhomogeneities in tracer distribution within the tumor mass, as well as the peripheral rim of tumor growth not made clearly visible by ^{99m}Tc-DTPA.

FIGURE 4. Immunohistochemistry with monoclonal antibody BC-1 is shown for a tumor section obtained from Patient AD01 (glioma) from the peripheral rim of tumor growth, where the most intense ^{99m}Tc-BC-1 uptake had been observed. Strong expression of oncofetal fibronectin around a pathologic blood vessel formed at the edge of tumor infiltration in the normal brain tissue is shown by the intense red staining.

utilized in the current study (patients with brain tumors) were obviously not selected with a diagnostic perspective in mind for this particular patient population, but simply to determine whether the well-known intense neoangiogenesis taking place in these tumors could be targeted with the radiolabeled MoAb BC-1.

The scintigraphic observations made during this study show that, upon injection of ^{99m}Tc-BC-1, deposition of radioactivity within the brain tumor mass is a more accurate indicator of the pattern of peripheral tumor growth than of simple disruption of the blood-brain barrier. This conclusion was further supported by immunohistochemical analysis of the tumor specimens, which showed greater expression of oncofetal fibronectin at the peripheral rim of tumor growth that was highly consistent with the pattern of ^{99m}Tc-BC-1 uptake. Failure of the modified immunohistochemical procedure to actually detect in vivo deposition of the MoAb tracer in the tumor sections was most likely due to the intrinsically low sensitivity of such a technique, considering that patients received extremely low amounts of radiolabeled antibody (only 200 μg per patient).

Another noteworthy observation of this study was the relatively slow plasma clearance of radiolabeled MoAb BC-1. In fact, a terminal $T_{1/2}$ of about 30 hours is relatively long for a ^{99m}Tc-labeled MoAb tracer, as conjugation of the antibody molecule with a chelating agent (a common prerequisite for most ^{99m}Tc-labeling procedures) can induce some conformational protein changes that usually result in shortened in vivo survival. The pharmacokinetic pattern observed with ^{99m}Tc-BC-1 is consistent with the results obtained in an animal model of in vivo tumor targeting, in which MoAb BC-1 was labeled either with iodine-125 or with the infrared fluorophore, CY7-bis(N-hydroxy-succinimido)-ester.[1] In this regard, and particularly for diagnostic applications in patients with cancers located outside the brain, the use of antioncofetal fibronectin fragments with faster blood clearance, such as those obtained by ^{99m}Tc labeling of binding sequences produced by recombinant techniques,[16] may represent a key issue in achieving favorable tumor-to-background ratios (and therefore efficient tumor imaging) early after injection of a ^{99m}Tc-labeled tracer.

The favorable results obtained in this phase of the study encourage further investigations aimed at assessing the in vivo tumor targeting capabilities of MoAb BC-1. Such investigations should address, first of all, the issue of diagnostic imaging applications in areas outside the brain, to avoid the confounding factor represented by the blood-brain disruption. A subsequent phase might explore the therapeutic potential of MoAb BC-1, pursuing the possibility of delivering sufficient radiation doses to molecular targets that are not only interspersed amidst the tumor mass, but also preferentially distributed within and around neoformed vessels that support tumor growth.[17]

REFERENCES

1. Mariani G, Lasku A, Balza E, Gaggero B, Motta C, Di Luca L, et al. Tumor targeting potential of the monoclonal antibody BC-1 against oncofetal fibronectin in nude mice bearing human tumor implants. *Cancer* 1997;80:2378–84.
2. Norton PA, Hynes RO. Alternative splicing of chicken fibronectin in embryos and in normal and transformed cells. *Mol Cell Biol* 1987;7:4297–307.
3. Zardi L, Carnemolla B, Siri A, Petersen TE, Paolella G, Sebastio G, et al. Transformed human cells produce a new fibronectin isoform by preferential alternative splicing of a previously unobserved exon. *EMBO J* 1987;6:2337–42.
4. Carnemolla B, Balza E, Siri A, Zardi L, Nicotra MR, Bigotti A, et al. A tumor-associated fibronectin isoform generated by alternative splicing of messenger RNA precursors. *J Cell Biol* 1989;108:1139–48.
5. Ffrench-Constant C, Van de Water L, Dvorak HF, Hynes RO. Reappearance of an embryonic pattern of fibronectin splicing during wound healing in the adult rat. *J Cell Biol* 1989;109:903–14.
6. Borsi L, Balza E, Allemanni G, Zardi L. Differential expression of the fibronectin isoform containing the ED-B oncofetal domain in normal human fibroblast cell lines originating from different tissues. *Exp Cell Res* 1992;199:98–105.
7. Carnemolla B, Leprini A, Allemanni G, Saginati M, Zardi L. The inclusion of the type III repeat ED-B in the fibronectin molecule generates conformational modifications that unmask a cryptic sequence. *J Biol Chem* 1992;267:24689–92.
8. Castellani P, Viale G, Dorcaratto A, Nicolò G, Kaczmarek J, Querzé G, et al. The fibronectin isoform containing the ED-B oncofetal domain: a marker of angiogenesis. *Int J Cancer* 1994;59:612–8.
9. Kaczmarek J, Castellani P, Nicolò G, Spina B, Allemanni G, Zardi L. Distribution of oncofetal fibronectin isoforms in normal, hyperplastic, and neoplastic human breast tissues. *Int J Cancer* 1994;58:11–6.
10. Ruoslahti E. Structure and biology of proteoglycans. *Ann Cell Biol* 1988;4:229–55.
11. Hynes RO. Fibronectins. New York: Springer-Verlag, Inc., 1990.
12. Castellani P, Siri A, Rosellini C, Infusini E, Borsi L, Zardi L. Transformed human cells release different fibronectin variants than do normal cells. *J Cell Biol* 1986;103:1671–7.
13. Borsi L, Carnemolla B, Castellani P, Rosellini C, Vecchio D, Allemanni G, et al. Monoclonal antibodies in the analysis of fibronectin isoforms generated by alternative splicing of mRNA precursors in normal and transformed human cells. *J Cell Biol* 1987;104:595–600.
14. Vartio T, Laitinen L, Narvanen O, Cutolo M, Thornell LE, Zardi L, et al. Differential expression of the ED sequence-containing form of cellular fibronectin in embryonic and adult human tissues. *J Cell Sci* 1987;88:419–30.
15. Oyama F, Hirohashi S, Shimosato Y, Titani K, Sekiguchi K. Deregulation of alternative splicing of fibronectin pre-mRNA in malignant human liver tumors. *J Biol Chem* 1989;264:10331–4.
16. Liberatore M, Neri D, Neri G, Pini A, Iurilli AP, Ponzo F, et al. Efficient one-step direct labelling of recombinant antibodies with technetium-99m. *Eur J Nucl Med* 1995;22:1326–9.
17. Bicknell R, Harris AL. Mechanisms and therapeutic implications of angiogenesis. *Curr Opin Oncol* 1996;8:60–5.